A General Sampling Theory for Nonideal Acquisition Devices

Michael Unser, *Senior Member, IEEE,* and Akram Aldroubi

***Abstract*—We first describe the general class of approximation spaces generated by translation of a function $\varphi(x)$, and provide a full characterization of their basis functions. We then present a general sampling theorem for computing the approximation of signals in these subspaces based on a simple consistency principle. The theory puts no restrictions on the system input which can be an arbitrary finite energy signal; bandlimitedness is not required. In contrast to previous approaches, this formulation allows for an independent specification of the sampling (analysis) and approximation (synthesis) spaces. In particular, when both spaces are identical, the theorem provides a simple procedure for obtaining the least squares approximation of a signal. We discuss the properties of this new sampling procedure and present some examples of applications involving bandlimited, and polynomial spline signal representations. We also define a spectral coherence function that measures the "similarity" between the sampling and approximation spaces, and derive a relative performance bound for the comparison with the least squares solution.**

I. INTRODUCTION

SAMPLING is the process of representing functions of a continuous variable x by sequences of numbers (discrete signal representation). A classical approach to this problem is provided by Shannon's sampling theorem which states that a bandlimited function $\tilde{g}(x)$ is entirely characterized by its samples taken at an appropriate rate [1]–[3]. The corresponding sampling/reconstruction procedure is described by the block diagram in Fig. 1(a), where $\eta(x) = \text{sinc}(x)$ is the interpolation kernel. Similar interpolation schemes have also been defined for other function spaces, including bandpass functions [4], and polynomial splines [5]–[7].

If the functions to be processed are not bandlimited (e.g., $g(x) \in L_2$), the standard procedure is to use an additional prefiltering module (ideal low-pass filter), which acts by suppressing aliasing (cf. Fig. 1(b) with $\mathring{\varphi}(x) = \text{sinc}(x)$) [1], [8]. The corresponding bandlimited reconstruction $\tilde{g}(x)$ then turns out to be the orthogonal projection of $g(x)$ on the subspace of bandlimited functions. This observation suggests a second interpretation of the sampling process as an approximation procedure. This point of view has led to the formulation of least squares sampling theories for polynomial splines [9], [10], as well as for more general classes of functions generated from the integer translates of a generating kernel $\varphi(x)$ (to be defined in Section II-A) [11]. A related development is Ogawa's generalized sampling theory for approximating functions in finite dimensional vector spaces [12], [13]. The principle of a minimum error signal approximation (orthogonal projection) is also used explicitly in the multiresolution formulation of the wavelet transform proposed by Stéphane Mallat [14], [15]. A property that is shared by all these representations is that the discrete expansion coefficients are obtained by simple inner product between the input signal $g(x)$ and an appropriate (biorthogonal) analysis function. At a fixed resolution, this process is equivalent to prefiltering the signal and sampling thereafter, as illustrated in Fig. 1(b). The optimal (least squares) prefilter $\mathring{\varphi}(-x)$ is uniquely specified by the approximation space [11] (cf. Table I on the next page); in the orthogonal case, it simply is the generating function itself.

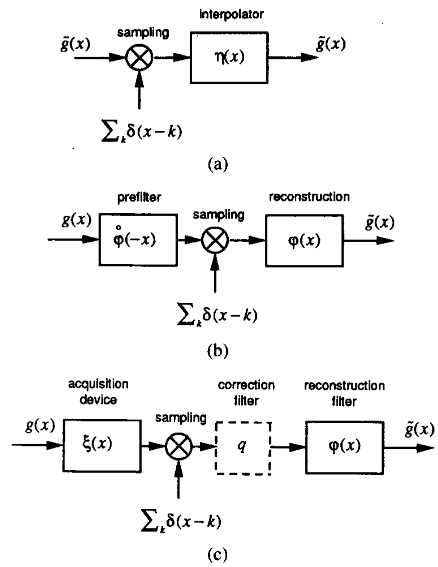

Fig. 1. Block diagram representation of three sampling procedures: (a) Interpolation; (b) least squares approximation; (c) sampling with nonideal acquisition device. The sampling operation is modeled by a multiplication with the sequence of Dirac impulses $\sum_{k\in Z} \delta(x-k)$. The solid rectangular boxes represent convolution operators (analog filters). The exact meaning of the symbols used is clarified at the end of Section I.

In most applications, the analysis function is given a priori and corresponds to the impulse response of the acquisition device, which we denote by $\xi(x)$. Clearly, the approximation error is minimized if and only if $\xi(x) = \mathring{\varphi}(-x)$; this situation corresponds to the case of an ideal (or optimal) acquisition device. If this condition is not satisfied, different types of errors

Manuscript received September 23, 1992; revised March 29, 1994. The associate editor coordinating the review of this paper and approving it for publication was Prof. Russell M. Mersereau.

The authors are with the Biomedical Engineering and Instrumentation Program, National Center for Research Resources, National Institutes of Health, Bethesda, MD 20892 USA.

IEEE Log Number 9404807.

1053-587X/94$04.00 © 1994 IEEE

(distortion, aliasing) are introduced into the discretization process; this may result in a significant loss of performance.

In this paper, we address this problem and propose a corrective procedure that takes the form of a digital filter. For this purpose, we develop a new sampling theory that offers the flexibility of an independent specification of the sampling (or analysis) and approximation (or synthesis) spaces. The corresponding system is shown in Fig. 1(c); it includes a model of the acquisition device as well as a digital deconvolution filter q. The generating kernel φ in the post-filtering module specifies the approximation space. It may also represent the impulse response of a particular physical reconstruction device.

The present theory is based on a simple consistency principle. The basic requirement is that the resulting signal approximation $\tilde{g}(x)$ if re-injected into the system must result in the same measurements as the original signal itself. As far as the sensing device is concerned, the signal and its approximation are therefore equivalent. We will see that this formulation is quite general in the sense that it includes conventional and least squares sampling procedures as particular cases. An implication of these results is a restatement of Shannon's sampling theorem for nonideal acquisition devices: under suitable conditions (i.e., the invertibility of a given discrete convolution operator), a bandlimited function $\tilde{g}(x)$ (or, by extension, $\tilde{g}(x) \in V$ where V is the representation space) is completely determined from its measured sample values $\xi * \tilde{g}(x)|_{x=k}$. This also means that the function $\tilde{g}(x)$ can be recovered without any loss from its measurements.

The presentation is organized as follows. In Section II, we define the relevant approximation spaces, and give a complete characterization of their basis functions. The general sampling theory corresponding to the block diagram in Fig. 1(c) is derived in Section III. We also define a spectral coherence function that provides a measure of the discrepancy between the sampling and approximation spaces. In Section IV, we consider the issue of performance and derive a theoretical bound that allows the worst case comparison with the optimal (but non-realizable) least squares solution. Finally, in Section V, we consider some examples of application. These include a new formulation of the standard deconvolution problem, and several examples involving bandlimited and polynomial spline representations of signals.

A. Notations and Operators

L_2 is the space of measurable, square-integrable, real-valued functions $g(x), x \in R$. L_2 is a Hilbert space whose metric $\|\cdot\|$ (the L_2-norm) is derived from the inner product

$$\langle g, h \rangle = \langle g(x), h(x) \rangle = \int_{-\infty}^{+\infty} g(x)h(x)dx \quad (1)$$

$$\|g\| = \sqrt{\langle g, g \rangle} = \left(\int_{-\infty}^{+\infty} |g(x)|^2 dx \right)^{\frac{1}{2}}. \quad (2)$$

The basic (or generic) generating function of a subspace $V \subset L_2$ is denoted by φ; i.e., $V(\varphi) = \text{span}\{\varphi(x-k)\}_{k \in Z}$. Occasionally, we will use another Greek letter to indicate a certain characteristic property, as specified in Table I. The symbol "$^{\circ}$" is used to represent the dual (or biorthogonal)

TABLE I
VARIOUS TYPES OF EQUIVALENT GENERATING FUNCTIONS WITH THEIR SPECIFIC PROPERTIES

Type	Symbol	Fourier transform of the weighting sequence p	Property
Basic or generic	$\varphi(x)$	$\hat{p}(f) = 1$	Admissibility: $0 < A \le \sum_{i \in Z} \lvert\hat{\varphi}(f-i)\rvert^2 \le B$
Cardinal or interpolating	$\eta(x)$	$\hat{p}_c(f) = \frac{1}{\sum_{i \in Z} \hat{\varphi}(f-i)}$	Interpolation: $\eta(k) = \delta_k$
Orthogonal	$\phi(x)$	$\hat{p}_o(f) = \frac{1}{\sqrt{\sum_{i \in Z} \lvert\hat{\varphi}(f-i)\rvert^2}}$	Orthogonality: $\langle \phi_k, \phi_l \rangle = \delta_{k,l}$
Dual	$\mathring{\varphi}(x)$	$\hat{p}_d(f) = \frac{1}{\sum_{i \in Z} \lvert\hat{\varphi}(f-i)\rvert^2}$	Biorthogonality: $\langle \mathring{\varphi}_k, \varphi_l \rangle = \delta_{k,l}$

operator. An approximation in V of the function $g \in L_2$ is usually denoted by $\tilde{g}$; the same notation may also be used to indicate that the function is already included in the approximation space (cf. Fig. 1(a)).

l_2 is the vector space of square-summable sequences (or discrete signals) $a(k), k \in Z$. The convolution between two sequences a and b is denoted by $b * a(k)$. The sequence $b(k)$ can be viewed as a discrete convolution operator (or digital filter) that is applied to the signal $a \in l_2$. This filter is characterized by its transfer function $\hat{b}(f) = \sum_{k \in Z} b(k) e^{-j2\pi kf}$. An important result concerning the stability and the reversibility of such operators is given by the following proposition (cf. [11]).

Proposition 1: A sequence $b(k)$ defines an invertible discrete convolution operator from l_2 into itself if and only if there exists two positive constants m and M such that $m \le |\hat{b}(f)| \le M$, almost everywhere (a.e.).

This condition insures the existence and stability of the inverse filter, which we denote by

$$(b)^{-1}(k) \stackrel{\text{Fourier}}{\longleftrightarrow} 1/\hat{b}(f). \quad (3)$$

If in addition b is symmetrical, we can also define its square-root convolution inverse

$$(b)^{-1/2}(k) \stackrel{\text{Fourier}}{\longleftrightarrow} 1/\sqrt{\hat{b}(f)}. \quad (4)$$

II. PRELIMINARY NOTIONS

In this section, we first define the notion of "shift-invariant" approximation space and give the necessary and sufficient conditions for such a construction. We then indicate a general procedure for generating equivalent sets of basis functions.

A. Subspaces Generated by Integer Translates

The purpose of discretization is to represent a function $g(x)$ of the continuous variable x by a discrete sequence of samples. Such a discrete signal representation is often better suited for signal processing and for data transmission. In order to define a coherent sampling procedure, we first have to select a subset (or subspace) of functions entirely characterized by such a sequence of coefficients.

Without loss of generality, we assume that the sampling step is one. Further, we require our sampling procedure to be invariant with respect to integer translates. This implies that our signal representation must also be shift-invariant.

Accordingly, we can specify our prototype function space V, as in [11]

$$V=\left\{h(x)=\sum_{k\in Z}c(k)\varphi(x-k),\ c\in l_2\right\} \tag{5}$$

where $\varphi(x)$ is the *generating* function. The only restriction on the choice of the generating function is that the integer translates of φ define a Riesz basis[1] of V. This insures that V is a well-defined (closed) subspace of L_2 and that the process of approximating a function g in V makes sense. Practically, this mathematical requirement translates into a relatively simple condition on $\hat{\varphi}(f)$, the Fourier transform of $\varphi(x)$.

Proposition 2: $\{\varphi(x-k)\}_{k\in Z}$ is a Riesz basis of $V\subset L_2$ if and only if $A\leq\sum_{i\in Z}|\hat{\varphi}(f-i)|^2\leq B$, a.e., where A and B are two strictly positive constants.

A proof of this result is given in [11]. Note that the central term in the inequality represents the Fourier transform of the sampled autocorrelation sequence

$$a(k)=\langle\varphi(x),\varphi(x-k)\rangle \overset{\text{Fourier}}{\longleftrightarrow} \hat{a}(f)=\sum_{i\in Z}|\hat{\varphi}(f-i)|^2. \tag{6}$$

Hence, the admissibility condition in Proposition 2 is equivalent to the requirement that $a(k)$ defines an invertible convolution operator from l_2 into itself (cf. Proposition 1).

The class of functions that can be constructed by a generating kernel as in (5) is quite general. For instance, if we choose $\varphi(x)=\mathrm{sinc}(x)$, we get the subspace of functions in L_2 that are bandlimited to $f\in[-\frac{1}{2},\frac{1}{2}]$. This is precisely the class of functions considered in Shannon's Sampling Theorem [1]. The corresponding frame constants in Proposition 2 are $A=B=1$, which reflects the property that the sinc basis is orthogonal.

Another choice is $\varphi(x)=\beta^n(x)$, where $\beta^n(x)$ is Schoenberg's central B-spline of order n [6], [7]. These kernels are constructed recursively by repeated convolution of a B-spline of order 0

$$\beta^n(x)=\beta^0*\beta^{n-1}(x) \overset{\text{Fourier}}{\longleftrightarrow} \mathrm{sinc}^{n+1}(f) \tag{7}$$

where $\beta^0(x)$ is the characteristic function in the interval $[-\frac{1}{2},\frac{1}{2})$. In this case, $\varphi(x)$ generates the basic space of polynomial splines of order n. These functions are polynomials of degree n within each interval $[k-\frac{1}{2},k+\frac{1}{2}), k\in Z$ when n is even, and $[k,k+1), k\in Z$ when n is odd, with the constraint that the segments are connected in a way that insures the continuity of all derivatives up to order $n-1$. For $n=0$ (resp., $n=1$), we have the simple family of piecewise constant (resp. linear) functions.

Another special case occurs in the context of the wavelet transform where φ may represent any valid scaling or wavelet function. This connection is further discussed in [16].

[1]By definition, a set $\{e_i\}_{i\in Z}$ of the Hilbert space $H=\mathrm{span}\{e_i\}_{i\in Z}$ is a Riesz basis if there exist two positive constants A and B such that: $\forall c\in l_2, A\cdot\|c\|_{l_2}^2\leq\|\sum_{i\in Z}c(i)e_i\|^2\leq B\cdot\|c\|_{l_2}^2$

B. Equivalent Basis Functions

$\varphi(x)$ is not the only function that generates the generic signal subspace V defined by (5). In fact, alternative sets of shift-invariant basis functions can be constructed by suitable linear combination, a property that is expressed by the following proposition.

Proposition 3 [11]*:* $\lambda(x)=\sum_{k\in Z}p(k)\varphi(x-k)$ is an equivalent generating function of $V\subset L_2$ iff. p is an invertible convolution operator from l_2 into l_2.

In fact, the operator p can be chosen so that the basis functions satisfy certain prescribed properties. The details of such a construction can be found in [11]. A summarized description of the main types of generating functions is given in Table I. For each set of basis functions, there is a unique set of coefficients that characterizes the function $h\in V$. The selection of the most appropriate representation generally depends the application.

A good illustration of these concepts is provided by the example of polynomial splines [10], [17]. Some examples of such generating functions are shown in Fig. 2. Note that all the functions in solid lines are true interpolation kernels (i.e., they vanish for all integers except the origin where they take the value one). The B-spline of order 0 (Fig. 2(a)) and the sinc function (Fig. 2(d)) are also orthogonal.

Here, in addition to the basic expansion, we will use the orthogonal representation of a function $h\in V$

$$h=\sum_{k\in Z}c(k)\varphi_k=\sum_{k\in Z}d(k)\phi_k \tag{8}$$

with the short form convention: $\varphi_k=\varphi(x-k)$. The orthogonal generating function is given by

$$\phi(x)=\sum_{k=-\infty}^{+\infty}(a)^{-1/2}(k)\varphi(x-k) \tag{9}$$

where $(a)^{-1/2}$ is the square-root convolution inverse (cf. (4)) of the autocorrelation sequence a defined by (6). The property of the orthogonal representation that is the most important for our purpose is that the L_2-norm of a signal $h\in V$ is also equal to the l_2-norm of its coefficients in the orthogonal representation; i.e.

$$\|h\|_{L_2}=\|d\|_{l_2}=\sqrt{\sum_{k=-\infty}^{+\infty}d^2(k)}. \tag{10}$$

III. General Sampling Theory

The orthogonal projection of a given function $g\in L_2$ on V provides the optimal representation in the sense that the L_2-approximation error is minimized. Moreover, this least squares solution can be computed simply by prefiltering and sampling [11]. The corresponding optimal prefilter $\mathring{\varphi}\in V$ is uniquely specified and corresponds to the dual of the generating function φ (cf. Table I).

In practice, the prefilter (or sampling kernel) typically corresponds to the impulse response of the acquisition device. In most cases, this operator is specified a priori and it is therefore usually not possible to obtain the least squares solution

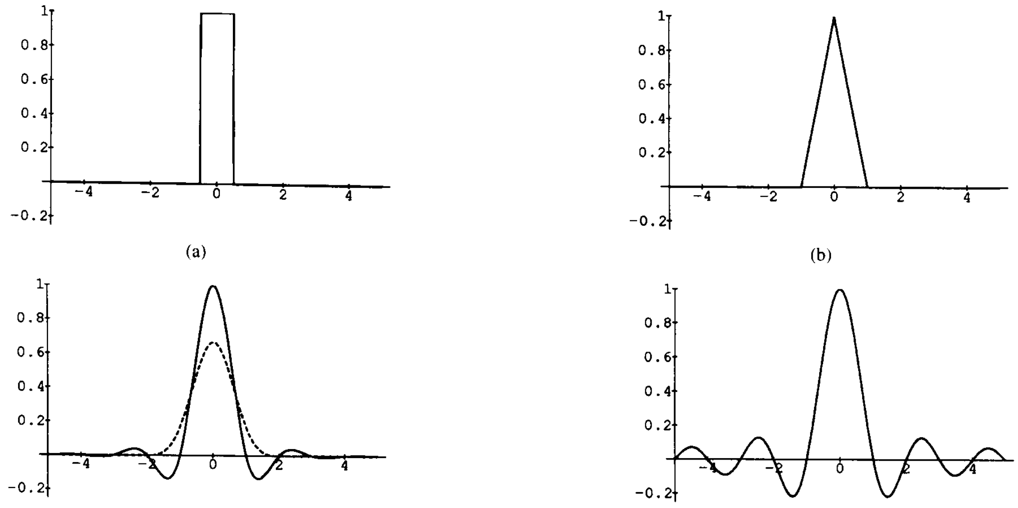

Fig. 2. Examples of polynomial spline basis functions. (a) B-spline of order 0, (b) B-spline of order 1, (c) cubic cardinal spline (solid line) and B-spline (dashed line), (d) cardinal sinc function ($n \to +\infty$). The B-splines and cardinal splines for $n = 0$ and $n = 1$ are identical.

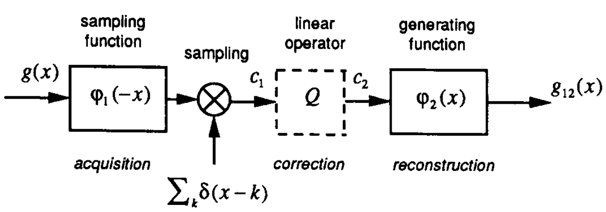

Fig. 3. General sampling block diagram.

directly. For this reason, we will consider a more general sampling procedure that allows an independent specification of the sampling space.

A. Axiomatic Formulation

Our system is schematically represented in Fig. 3. It will acquire uniformly spaced samples at the output of the acquisition device and produce an approximation $\tilde{g} \in V_2$ of the input function $g \in L_2$. The relevant parameters are:

- $\varphi_1(-x)$: the impulse response of acquisition device;
- Q: a linear deconvolution operator to be specified; and
- $\varphi_2(x)$: the generating function of the *approximation* space V_2.

We also introduce the notion of *sampling* space V_1 which is generated by φ_1. Both V_1 and V_2 are defined by an equation equivalent to (5); φ_1 and φ_2 both satisfy the admissibility condition in Proposition 2.

To specify the signal approximation $\tilde{g}$, we also introduce the following constraints on our system:

(i) linearity and shift-invariance for integer translates;
(ii) consistent measurements:

$$c_1(k) = \langle g(x), \varphi_1(x-k)\rangle = \langle \tilde{g}(x), \varphi_1(x-k)\rangle. \quad (11)$$

The first condition is a standard one. The second indicates that the signal g and its approximation $\tilde{g}$ are essentially equivalent, at least as far as the sensor is concerned. It also implies that the system globally acts as a projector.

Before stating our main result, we define the correlation sequences

$$a_{ij}(k) = \langle \varphi_i(x-k), \varphi_j(x)\rangle = \langle \varphi_{i,k}, \varphi_{j,0}\rangle, \quad (i,j = 1,2). \quad (12)$$

For $i = 1$ and $j = 2$, we get the sequence $a_{12}(k)$ which corresponds to the cross-correlation between the input and output sampling functions.

Theorem 1: A unique solution satisfying constraints (i) and (ii) exists iff $a_{12}(k)$ is an invertible convolution operator for l_2 into l_2. The solution is the projection of g on V_2 perpendicular to V_1

$$\tilde{g} = g_{12} = P_{2\perp 1}g = \sum_{k\in Z} c_2(k)\varphi_{2,k} \quad (13)$$

where $c_2(k) = (a_{12})^{-1} * c_1(k)$.

An implicit requirement for this result is that the sequence of measurements $c_1(k)$ is in l_2. This condition is insured by the admissibility constraint on the sampling function φ_1. This latter constraint can be dropped provided that the input signal g is sufficiently well behaved. An example in which φ_1 is a distribution is presented in Section V-B.

Theorem 1 can be applied directly to design of the correction filter in the block diagram in Fig. 1(c). Specifically, by using Poisson's summation formula, we obtain a simple expression for this filter in the Fourier domain

$$\hat{q}(f) = \frac{1}{\sum_{i\in Z} \hat{\varphi}_1^*(f-i)\hat{\varphi}_2(f-i)} = \frac{1}{\sum_{i\in Z} \hat{\xi}(f-i)\hat{\varphi}(f-i)} \quad (14)$$

where $\hat{\xi}(f)$ is the transfer function of the acquisition device ($\xi(x) = \varphi_1(-x)$), and where $\hat{\varphi}(f)$ is the Fourier transform of the generating function $\varphi(x) = \varphi_2(x)$.

Proof: Condition *(i)* implies that $c_2 = Qc_1$, where Q is a linear shift-invariant operator. This operator is therefore equivalent to a digital filter with an impulse response q. Hence, the function $\tilde{g}$ can be written as

$$\tilde{g}(x) = \sum_{k=-\infty}^{+\infty} (q * c_1)(k)\varphi_2(x-k). \tag{15}$$

If we reinject this function in our system, we get the following measurements

$$\begin{aligned} c_{21}(l) &= \langle \tilde{g}(x), \varphi_1(x-l)\rangle \\ &= \sum_{k=-\infty}^{+\infty} (q * c_1)(k)\langle \varphi_2(x-k), \varphi_1(x-l)\rangle \\ &= \sum_{k=-\infty}^{+\infty} (q * c_1)(k) a_{12}(l-k). \end{aligned} \tag{16}$$

By using this result together with condition *(ii)*, we have the equality

$$c_1(l) = q * a_{12} * c_1(l)$$

from which we deduce that $q = (a_{12})^{-1}$.

Equation (15) defines a linear operator P: $L_2 \rightarrow V_2$. To prove that P is the projection on V_2 perpendicular to V_1, we need to show that P has the following properties

$$\forall h \in V_2, \qquad Ph = h \tag{17}$$
$$\forall g \in L_2, \qquad g - Pg \in V_1^{\perp} \tag{18}$$
$$\forall e \in V_1^{\perp}, \qquad Pe = 0. \tag{19}$$

First, we represent the function $h \in V_2$ by its expansion

$$h = \sum_{l \in Z} c(l)\varphi_2(x-l).$$

Using (11) and (15), we can determine the expansion coefficients of Ph as follows

$$\begin{aligned} \sum_{k=-\infty}^{+\infty} (a_{12})^{-1} * \langle h, \varphi_1(x-k)\rangle &= \sum_{k=-\infty}^{+\infty} (a_{12})^{-1} * c * a_{12}(k) \\ &= c(k) \end{aligned}$$

which proves (17). At this point, we have established that P is a projector on V_2. Next, we consider the inner product

$$\langle g - Pg, \varphi_{1,k}\rangle = \langle g(x), \varphi_1(x-k)\rangle - \langle g_{12}(x), \varphi_1(x-k)\rangle.$$

Using (11) and (16) together with $q = (a_{12})^{-1}$, we find that

$$\langle g - g_{12}, \varphi_{1,k}\rangle = c_1(k) - (a_{12})^{-1} * a_{12} * c_1(k) = 0$$

which proves that the projection error is orthogonal to V_1 (cf. (18)). Finally, we can use the fact that

$$\forall e \in V_1^{\perp}, \langle e, \varphi_{1,k}\rangle = 0$$

which, together with (11) and (15), implies that (19) is satisfied as well. □

B. Discussion and Properties

The sampling procedure described by Theorem 1 turns out to be quite general. We will now identify some of its key properties:

1) Equivalent Biorthogonal Expansion: The output of the system described by Theorem 1 can also be represented as

$$\tilde{g} = \sum_{k \in Z} \langle g, \mathring{\varphi}_{12,k}\rangle \varphi_{2,k} \tag{20}$$

where the equivalent sampling function is given by

$$\mathring{\varphi}_{12}(x) = \sum_{k \in Z} (a_{12})^{-1}(k)\varphi_1(x-k). \tag{21}$$

The corresponding basis functions are biorthogonal in the sense that

$$\langle \mathring{\varphi}_{12,k}, \varphi_{2,l}\rangle = \delta_{k,l}. \tag{22}$$

The direct interpretation of this result is that the function $\varphi_2(x)$ (or any of its integer shifts) can be reconstructed exactly if it is injected into the system.

2) The Minimum Error Solution: If $V_1 = V_2$ then $\tilde{g} = P_2 g$ is the orthogonal projection of g onto V_2; this corresponds to the case of the least squares sampling theory developed in [11]. Therefore, the system provides the minimum error approximation $g \in L_2$ if and only if $\varphi_1 \in V_2$. In this special situation, the equivalent biorthogonal function (21) is precisely the dual of the generating function described in the last row of Table I, and the procedure is optimal. Otherwise, we will obtain an approximate solution, the quality of which depends on the "similarity" of the functions spaces V_1 and V_2. A detailed investigation of this issue will be given in Section IV.

3) The Connection with Shannon's Theory: We have already seen that the functions included in the approximation space V_2 are left unchanged (cf. (17)). An equivalent formulation of this property is that all functions $h \in V_2$ can be reconstructed without any loss from their sampled measured values. This statement is very similar to Shannon's original sampling theorem [1]; the main distinction is that we are now talking of measured values instead of signal samples. The class of functions considered here is also more general than the family of bandlimited signals.

4) Signal Approximation in the Sampling Space: The approximation of function g given by (13) contains all the information necessary to compute $P_1 g$, the projection of g on V_1. Specifically, we have that

$$\begin{aligned} \forall g \in L_2, P_1 g &= P_1 P_{2\perp 1} g \\ &= \sum_{k \in Z} (a_{11})^{-1} * a_{12} * c_2(k)\varphi_{1,k} \end{aligned} \tag{23}$$

where $c_2(k)$ are the expansion coefficients of $g_{12} = P_{2\perp 1} g$ in (13). The stability of the inverse filter $(a_{11})^{-1}$ is guaranteed by the fact that φ_1 satisfies the admissibility condition.

5) Extension to Higher Dimensions: The generalization of these results for higher dimensional signals such as images should not present any major difficulty. This extension is straightforward if both the sampling and generating functions are separable; i.e., they can be obtained from the product of

1-D functions defined for each index variable. In this case, all transformations are separable and the linear operator Q can be implemented by successive 1-D filtering along the coordinates.

C. Input/Output Coherence Measures

An important practical issue is how good the computable approximation $P_{2\perp 1}g$ is compared to the optimal least squares solution $P_2 g$. In order to provide a quantitative answer to this question, we now define an input-output coherence function that measures the "similarity" between the functions spaces V_1 and V_2.

Our initial assumptions on φ_1 and φ_2 insure that both a_{11} and a_{22} are invertible convolution operators. It is thus possible to construct the orthogonal sampling functions $\phi_1(x)$ and $\phi_2(x)$ defined by (9). We then compute a normalized form of the cross-correlation sequence $a_{12}(k)$ which is given by

$$r_{12}(k) = \langle \phi_1(x-k), \phi_2(x)\rangle = (a_{11})^{-1/2} * a_{12} * (a_{22})^{-1/2}(k). \tag{24}$$

Note that the sequence $r_{12}(k)$ also provides the orthogonal coefficients of the projection of ϕ_1 on V_2. Taking the Fourier transform, we obtain

$$\hat{r}_{12}(f) = \frac{\hat{a}_{12}(f)}{\sqrt{\hat{a}_{11}(f)\hat{a}_{22}(f)}}. \tag{25}$$

To get a measure that is symmetrical with respect to the indices 1 and 2, we take the modulus of $\hat{r}_{12}(f)$. This leads us to the definition of the *spectral coherence* function

$$|\hat{r}_{12}(f)| = \frac{\left|\sum_{k=-\infty}^{+\infty} \hat{\varphi}_1^*(f-k)\hat{\varphi}_2(f-k)\right|}{\sqrt{\sum_{k=-\infty}^{+\infty} |\hat{\varphi}_1(f-k)|^2}\sqrt{\sum_{k=-\infty}^{+\infty} \hat{\varphi}_2(f-k)|^2}} \tag{26}$$

which has been expressed as a function of the Fourier transforms of the kernels φ_1 and φ_2 using Poisson's summation formula. Note that this quantity takes the form of a correlation coefficient between the spectral components of ϕ_1 and ϕ_2. Some of the relevant properties of this function are listed in the following theorem:

Theorem 2: If the generating functions φ_1 and φ_2 satisfy the admissibility condition in Proposition 2, then the spectral coherence function defined by (26) has the following properties:

(i) $|\hat{r}_{12}(f)|$ is periodic and is independent of a particular choice of generating functions for the subspaces V_1 and V_2.
(ii) $|\hat{r}_{12}(f)| \leq 1, \forall f \in R$. Moreover, $|\hat{r}_{12}(f)| = 1, \forall f \in R$ if and only if $V_1 = V_2$.
(iii) If in addition φ_1 and φ_2 are in L_1 and their Fourier transforms both decay like $O(|f|^{-r}), r > \frac{1}{2}$, then $|\hat{r}_{12}(f)|$ is continuous.

The concept of equivalent generating functions is discussed in Section II-B. The interpretation of property (ii) in this context is that $|\hat{r}_{12}(f)|$ is invariant to changes of coordinate system.

The spectral coherence function can be used to compute an average measure of coherence between the subspaces V_1 and V_2

$$0 \leq \left(\int_0^1 |\hat{r}_{12}(f)|^2 df\right)^{1/2} = \|r_{12}\|_{l_2} \leq 1 \tag{27}$$

where the central equality is provided by Parseval's identity. In particular, it has the property that it is equal to one if and only if $V_1 = V_2$, in which case the approximations $g_{2\perp 1}$ and g_2 are equivalent (cf. Condition (ii) in Theorem 2). Note that $\|r_{12}\|$ also provides the L_2-norm of the projection of ϕ_1 on V_2 (cf. (24)).

D. Proof of Theorem 2

Property (i): The periodicity of $|\hat{r}_{12}(f)|$ follows from the periodicity of its individual terms. The invariance property can be verified simply by computing the spectral coherence for generalized generating functions $\lambda_1(x)$ and $\lambda_2(x)$ of the type defined in Proposition 3.

Property (ii): We write Schwarz inequality for a fixed value of f

$$\left|\sum_{k=-\infty}^{+\infty} \hat{\varphi}_1^*(f-k)\hat{\varphi}_2(f-k)\right|^2 \leq \left(\sum_{k=-\infty}^{+\infty} |\hat{\varphi}_1(f-k)|^2\right)\left(\sum_{k=-\infty}^{+\infty} |\hat{\varphi}_2(f-k)|^2\right)$$

which directly implies that $|\hat{r}_{12}(f)| \leq 1$. The equality holds for some frequency f_0 if and only if there exists a constant $\hat{p}$ (which depends on f_0) such that $\hat{\varphi}_1(f_0-k) = \hat{p}(f_0)\hat{\varphi}_2(f_0-k)$. The condition $\forall f \in [0,1], |\hat{r}_{12}(f)| = 1$ is therefore equivalent to

$$\forall k \in Z, \hat{\varphi}_1(f-k) = \hat{p}(f)\hat{\varphi}_2(f-k)$$

from which we conclude that $\hat{p}(f) = \hat{p}(f-k), \forall k \in Z$. This equation also implies that

$$\sum_{k=-\infty}^{+\infty} |\hat{\varphi}_1(f-k)|^2 = |\hat{p}(f)|^2 \sum_{k=-\infty}^{+\infty} |\hat{\varphi}_2(f-k)|^2.$$

Since φ_1 and φ_2 both satisfy the conditions in Proposition 2 with frame constants (A_1, B_1) and (A_2, B_2), we get the following inequality

$$0 < (A_1/B_2) \leq |\hat{p}(f)|^2 \leq (B_1/A_2)$$

which proves that $\hat{p}(f)$ is the Fourier transform of an invertible convolution operator on l_2 which we denote by p (cf. Proposition 1). Hence, we conclude that $\varphi_1(x) = \sum_{l\in Z} p(l)\varphi_2(x-l)$ and that the functions φ_1 and φ_2 generate the same subspace (cf. Proposition 3).

Property (iii): By the Riemann–Lebesgue Lemma, $\hat{\varphi}_1(f)$ and $\hat{\varphi}_2(f)$ are both continuous. If these functions also decay like $O(|f|^{-r})$ for some $r > 1/2$, then the series

$$\hat{a}_{ij}(f) \leq \sum_{k\in Z} |\hat{\varphi}_i^*(f-k)\hat{\varphi}_j(f-k)| \leq \text{const} \sum_{k=1}^{+\infty} |k|^{-2r}, i,j = 1,2,$$

are absolutely convergent independently of f. Thus, these series are continuous on [0, 1]. Since the terms in the denominator of (26) are nonvanishing, we conclude that $|\hat{r}_{12}(f)|$ is continuous as well. □

IV. Spectral Coherence And Error Estimates

It is clear from the previous results that if the acquisition device is such that $\varphi_1 \in V_2$ then the procedure described by Theorem 1 will indeed provide us with the minimum error approximation. Otherwise, we will obtain an approximate solution. In this section, we will derive a theoretical performance bound that corresponds to a worst case scenario. In order to state our main result (Theorem 3), we need to introduce several geometrical quantities that can be derived from the spectral coherence function defined above.

A. An Analogue of the Geometric Notion of Angle

Given two closed subspaces V_a and V_b of a Hilbert space H, we define the quantity

$$R(V_a, V_b) = \cos(\theta_R) = \inf_{u \in V_a \setminus \{0\}} \frac{\|P_b u\|}{\|u\|} \tag{28}$$

where P_b is the projection operator of H on V_b. This quantity provides a worst case estimate of the relative length reduction when a vector of V_a is projected on V_b. Using the analogy with conventional Euclidean geometry, we interpret the quantity θ_R as the largest angle between the subspaces V_a and V_b. We note, however, that $R(V_a, V_b)$ is not necessarily symmetrical with respect to the indices a and b.

In order to determine this quantity for the signal spaces V_1 and V_2, we use the orthogonal representations of a function g_1 and its projection $P_2 g_1$

$$g_1(x) = \sum_{k \in Z} d_1(k) \phi_{1,k} \tag{29}$$

$$P_2 g_1(x) = \sum_{k \in Z} d_{12}(k) \phi_{2,k}. \tag{30}$$

Using the linearity of the projection operator P_2 together with (24), we find that

$$\begin{aligned} P_2 g_1(x) &= \sum_{l \in Z} d_1(l) P_2 \phi_{1,l} \\ &= \sum_{l \in Z} d_1(l) \sum_{k \in Z} \langle \phi_{1,l}, \phi_{2,k} \rangle \phi_{2,k} = \sum_{k \in Z} r_{12} * d_1(k) \phi_{2,k}. \end{aligned}$$

It follows that the coefficients of $P_2 g_1$ in (30) are related to those in (29) by a simple convolution

$$d_{12}(k) = r_{12} * d_1(k) \tag{31}$$

where the operator r_{12} is the normalized cross-correlation sequence defined by (24). This equation corresponds to a product in the Fourier domain. Therefore, using (10) together with Parseval's identity, we get that

$$\begin{aligned} \|P_2 g_1\|^2 &= \int_0^1 |\hat{d}_{12}(f)|^2 df = \int_0^1 |\hat{r}_{12}(f)|^2 |\hat{d}_1(f)|^2 df \\ &\geq \left(\operatorname{ess} \inf_{f \in [0,1]} |\hat{r}_{12}(f)| \right)^2 \int_0^1 |\hat{d}_1(f)|^2 df \end{aligned} \tag{32}$$

$$\|g_1\|^2 = \int_0^1 |\hat{d}_1(f)|^2 df. \tag{33}$$

The next step is to minimize the ratio of these two quantities over all possible $\hat{d}_1$'s, which yields

$$\inf_{g_1 \in V_1 \setminus \{0\}} \frac{\|P_2 g_1\|}{\|g_1\|} = \rho_{12} := \operatorname{ess} \inf_{f \in [0, \frac{1}{2}]} |\hat{r}_{12}(f)|. \tag{34}$$

This lower bound is obtained by taking the *essential infimum* of the spectral coherence function defined by (26). If the requirements for condition (iii) in Theorem 2 are satisfied (i.e., $|\hat{r}_{12}(f)|$ is continuous in the interval [0, 1]), then the essential infimum reduces to the minimum of this function. We can also restrict the analysis to the interval [0, 1/2] since this function is symmetrical. Note that the bound given by (34) is symmetrical with respect to the indices 1 and 2 since $|\hat{r}_{12}(f)| = |\hat{r}_{21}(f)|$. Accordingly, we have that $R(V_1, V_2) = R(V_2, V_1) = \rho_{12}$, where ρ_{12} is entirely specified by the kernels φ_1 and φ_2 through (26) and (34).

B. Error Bound

An answer to the question of how close the approximation given by Theorem 1 is compared to the optimal least squares solution is provided by the following result.

Theorem 3: Let V_1 and V_2 be two closed subspaces of L_2 generated by φ_1 and φ_2, respectively. Then, for any $g \in L_2$,

$$1 \leq \sup_{g \in L_2} \left\{ \frac{\|g - g_{2\perp 1}\|}{\|g - g_2\|} \right\} \leq \frac{1}{\rho_{12}} = \frac{1}{\operatorname{ess\,inf}_{f \in [0,1/2]} |\hat{r}_{12}(f)|} \tag{35}$$

where $g_{2\perp 1} = P_{2\perp 1} g$ and $g_2 = P_2 g$ and where $|\hat{r}_{12}(f)|$ is given by (26).

It is important to keep in mind that the right hand side in (35) corresponds to the worst possible case and that this bound may not necessarily reflect what really happens in practice. A more realistic estimate of the error ratio may be $\|r_{12}\|^{-1}$ where $\|r_{12}\|$ is the global coherence measure defined by (27). This latter measure is an average performance index in the sense that it weights to all frequency components equally. It also corresponds to the case of an impulse or white noise signal. Further, we have the property that $\|r_{12}\| = 1$ if and only if $\rho_{12} = 1$.

As a corollary of Theorem 3, we get a measure of the maximum discrepancy between g_2 and $g_{2\perp 1}$

$$\sup_{g - g_{2\perp 1} \in V_1^{\perp} \setminus \{0\}} \frac{\|g_2 - g_{2\perp 1}\|}{\|g - g_{2\perp 1}\|} = \sqrt{1 - \rho_{12}^2}. \tag{36}$$

In particular, we note that if $\rho_{12} = 1$ (or, equivalently, $\|r_{12}\| = 1$) then $\|g_2 - g_{2\perp 1}\| = 0$, which means that the corresponding approximations $g_{2\perp 1}$ and g_2 are equivalent.

C. Proof of Theorem 3 and Related Results

The proof of Theorem 3 uses an argument that is almost purely geometrical and can be understood intuitively from the schematic representation in Fig. 4. We start with some preliminary results and definitions for the geometry of Hilbert spaces in general.

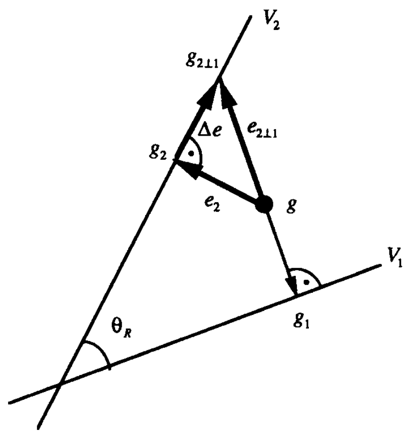

Fig. 4. Graphical representations of the various approximations and errors in the simplified case of one-component signal spaces.

Proposition 4: Let V be a closed subspace of the Hilbert space H. Then, for all $z \in H$

$$\sup_{u \in V\backslash\{0\}} \frac{\langle z, u\rangle}{\|u\|} = \|Pz\| \tag{37}$$

where P is the orthogonal projection of H onto V.

Given two closed subspaces V_a and V_b of the Hilbert space H, we define the quantity

$$S(V_a, V_b) = \cos(\theta_S) = \sup_{u \in V_a\backslash\{0\}} \frac{\|P_b u\|}{\|u\|} \tag{38}$$

where P_b is the orthogonal projection of H onto V_b. Again, using the analogy with Euclidean geometry, we interpret θ_S as the small angle between the subspaces V_a and V_b. Unlike the large angle defined by (28), the small angle is always symmetrical with respect to the indices a and b:

Proposition 5:

$$S(V_a, V_b) = S(V_b, V_a) = \sup_{\substack{u \in V_a\backslash\{0\} \\ u \in V_b\backslash\{0\}}} \left\{\frac{\langle u, v\rangle}{\|u\| \cdot \|\nu\|}\right\}.$$

The proof of this result directly follows from the application of Proposition 4 with ($V = V_a$ and $z \in V_b$) and ($V = V_b$ and $z \in V_a$), respectively.

We also need the following Lemma which relates the large angle between two subspaces to the angle between their orthogonal complements.

Lemma 1: Let V_a and V_b be two closed subspaces of the Hilbert space H. Then

$$R(V_a, V_b) = R(V_b^\perp, V_a^\perp) \tag{39}$$

where the quantity R is defined by (28).

Proof of Proposition 4: Using the Projection Theorem, we have that

$$\langle z, u\rangle = \langle Pz + \Delta z, u\rangle$$

where $Pz \in V$ and $\Delta z \in V^\perp$. Clearly, since the vectors $u \in V$ and $\Delta z \in V^\perp$ are orthogonal, we get

$$\frac{\langle z, u\rangle}{\|u\|} = \frac{\langle Pz, u\rangle}{\|u\|}.$$

Equation (37) then directly follows from the Schwarz inequality. Note that the maximum is attained when the unit vector $u/\|u\|$ is precisely in the direction of Pz. □

Proof of Lemma 1: Let us consider a vector $z \in H\backslash\{0\}$, which we decompose as

$$z = Pz + (I - P)z$$

where P is the orthogonal projection of H onto a closed subspace V. From the properties of projectors, we have that $Pz \in V$ and $(I - P)z \in V^\perp$. Hence, we can use the Pythagorean relation to show that

$$\frac{\|(I - P)z\|}{\|z\|} = \sqrt{1 - \left(\frac{\|Pz\|}{\|z\|}\right)^2}. \tag{40}$$

Clearly, maximizing the left hand side in this equation is equivalent to minimizing the last term inside the square root, and vice versa. By taking $z \in V_a\backslash\{0\}$ and $P = P_b$ in (40), it is not difficult to show that

$$\sup_{z \in V_a^\perp\backslash\{0\}} \frac{\|(I - P_b)z\|}{\|z\|} = S(V_a, V_b^\perp) = \sqrt{1 - R^2(V_a, V_b)}. \tag{41}$$

Similarly, by taking $z \in V_b^\perp\backslash\{0\}$ and $P = P_a$ in (40), we obtain

$$\inf_{z \in V_b^\perp\backslash\{0\}} \frac{\|(I - P_a)z\|}{\|z\|} = R(V_b^\perp, V_a^\perp) = \sqrt{1 - S^2(V_b^\perp, V_a)}. \tag{42}$$

From Proposition 5, we know that $S(V_b^\perp, V_a) = S(V_a, V_b^\perp)$. Hence, we can substitute the right hand side of (41) into (42), which finally yields (39) since $R(V_a, V_b)$ is positive. □

Proof of Theorem 3: We first define the following errors

$$\begin{cases} e_{2\perp 1} = g_{2\perp 1} - g \\ e_2 = g_2 - g \\ \Delta e = g_{2\perp 1} - g_2 \end{cases} \tag{43}$$

where $e_{2\perp 1} \in V_1^\perp$, $e_2 \in V_2^\perp$ and $\Delta e \in V_2$, respectively. A simplified graphical representation of these quantities is given in Fig. 4. Clearly, $e_{2\perp 1} = \Delta e + e_2$, where Δe and e_2 are both orthogonal. It follows from the Projection Theorem that

$$\Delta e = P_2 e_{2\perp 1} \tag{44}$$

$$e_2 = (I - P_2)e_{2\perp 1} \tag{45}$$

which is also equivalent to say that e_2 is the orthogonal projection of $e_{2\perp 1} \in V_1^\perp$ on $V_2^\perp$. Hence, we have that

$$\inf_{e_{2\perp 1} \in V_1^\perp\backslash\{0\}} \frac{\|e_2\|}{\|e_{2\perp 1}\|} = \inf_{e_{2\perp 1} \in V_1^\perp\backslash\{0\}} \frac{\|(I - P_2)e_{2\perp 1}\|}{\|e_{2\perp 1}\|} = R(V_1^\perp, V_2^\perp)$$

By using Lemma 1, we get

$$\inf_{e_{2\perp 1} \in V_1^\perp\backslash\{0\}} \frac{\|e_2\|}{\|e_{2\perp 1}\|} = R(V_2, V_1)$$

which, together with (34), yields the left hand side inequality in (35). The right hand side inequality simply follows from the fact that $\|g - P_2 g\| \le \|g - h\|, \forall h \in V_2$. □

To establish the corollary (36), we consider (44) and note that

$$\sup_{e_{2\perp 1}\in V_1^{\perp}\setminus\{0\}} \frac{\|\Delta e\|}{\|e_{2\perp 1}\|} = S(V_1^{\perp}, V_2) = S(V_2, V_1^{\perp})$$

where the right hand side follows from Proposition 5. The result then directly follows from (41) by taking $V_a = V_2$ and $P_b = P_1$.

V. Examples of Applications

We now present some examples that illustrate the theory and concepts discussed in the previous sections.

A. The Basic Deconvolution Problem

We first show that the present theory provides an alternative formulation of the basic deconvolution (or inverse filtering) problem. For this purpose, we consider an acquisition device with an impulse response $\xi(x) = \varphi_1(-x)$ and assume that the reconstruction is bandlimited with $\varphi_2(x) = \mathrm{sinc}(x)$. The discrete Fourier transform of the correction filter specified by Theorem 1 is given by

$$\hat{q}(f) = \frac{1}{\hat{\varphi}_1^*(f)}, \qquad f \in \left[-\frac{1}{2}, \frac{1}{2}\right]. \tag{46}$$

Note that this result is identical to the traditional inverse filter solution [18], [19]. Clearly, this operator is stable provided that the frequency response of the acquisition device $\hat{\xi}(f) = \hat{\varphi}_1^*(f)$ has no zeros in the frequency interval $[-\frac{1}{2}, \frac{1}{2}]$.

If φ_1 satisfies the admissibility condition, we can compute the spectral coherence function

$$|\hat{r}_{12}(f)| = \frac{|\hat{\varphi}_1(f)|}{\sqrt{\sum_{k=-\infty}^{+\infty} |\hat{\varphi}_1(f-k)|^2}}, \qquad f \in \left[-\frac{1}{2}, \frac{1}{2}\right]. \tag{47}$$

Note that this formula is identical to that of the frequency response of the orthogonalized sampling function ϕ_1 defined by (9). If φ_1 is bandlimited (i.e., $\varphi_1 \in V_2$) then $|\hat{r}_{12}(f)| = 1$, in which case a perfect signal recovery is possible. Otherwise, our theoretical results indicate that the ideal bandlimited signal approximation g_2 can, in general, not be obtained exactly from the samples, unless the input signal g is itself bandlimited (cf. Property (17)).

B. Interpolative Signal Model

In the absence of a priori knowledge, the simplest choice for $\varphi_1(x)$ is the Dirac delta function $\delta(x)$ (ideal sampling device). In this case, φ_1 is an element of S' (the space of tempered distributions), and is no longer an admissible generating function in the sense defined by Proposition 2. A sufficient condition for c_1 to be in l_2 is that the input signal g is continuous and decays sufficiently fast (e.g., $g(x) = O(|x|^{-r}, r > \frac{1}{2})$.

The appropriate correction filter then corresponds to the convolution inverse of the sampled generating function; i.e.

$$\hat{q}(f) = \frac{1}{\sum_{i\in Z} \hat{\varphi}_2(f-i)}. \tag{48}$$

Interestingly enough, this solution leads to a signal model that provides a perfect interpolation of our discrete input signal; i.e., $\tilde{g}(x)|_{x=k} = g(k)$. The system is therefore globally equivalent to the block diagram in Fig. 1(a). The impulse response of this interpolator is precisely the cardinal function $\eta(x)$ that is described in Table I.

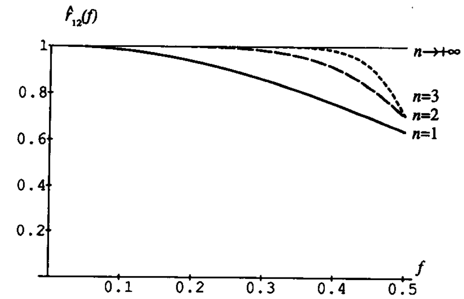

Fig. 5. Spectral coherence function $|\hat{r}_{12}(f)|$ between $\varphi_1(x) = \mathrm{sinc}(x)$ and $\varphi_2(x) = \beta^n(x)$, for n = 0, 1, and 3.

C. Bandlimited Acquisition and Spline Reconstruction

Another interesting combination is $\varphi_1(x) = \mathrm{sinc}(x)$ and $\varphi_2(x) = \beta^n(x)$, which corresponds to an ideal acquisition device and a signal approximation using polynomial splines of order n. Using (7) and (26), it is not difficult to show that the corresponding spectral coherence function is given by

$$\hat{r}_{12}(f) = \frac{\mathrm{sinc}^{n+1}(f)}{\sqrt{\sum_{k=-\infty}^{+\infty} \mathrm{sinc}^{2n+2}(f-k)}}, \qquad f \in \left[\frac{1}{2}, \frac{1}{2}\right]. \tag{49}$$

The right hand side term in this equation is also identical to the Fourier transform of the orthogonal spline basis functions considered in [10]. The graph of this function for different values of n is given in Fig. 5. Table II provides the corresponding values of the worst case and average coherence measures ρ_{12} and $\|r_{12}\|$. These results clearly indicate that the quality of the approximation improves with increasing order n. This tendency, however, is not reflected by the value of the worst case bound, since the minimum of $\hat{r}_{12}(f)$, which occurs at $f = 1/2$, remains approximately constant, irrespective of the value of n. We can use Theorem 3 in [10] to obtain the asymptotic behavior of $\hat{r}_{12}(f)$ as the order of the spline tends to infinity

$$\lim_{n\to+\infty} \{\hat{r}_{12}(f)\} = \begin{cases} 1, & f \in (-\frac{1}{2}, \frac{1}{2}) \\ 1/\sqrt{2}, & f = \pm\frac{1}{2} \end{cases}. \tag{50}$$

This convergence result implies that

$$\lim_{n\to+\infty} \left\{ \left(\int_0^1 |\hat{r}_{12}(f)|^2 df \right)^{1/2} \right\} = \lim_{n\to+\infty} \{\|r_{12}\|_{l_2}\} = 1. \tag{51}$$

This is a way of indicating that the subspaces of bandlimited and polynomial spline functions are essentially equivalent as the order of the spline goes to infinity. This property is consistent with a number of theoretical results reported earlier [5], [20], [21].

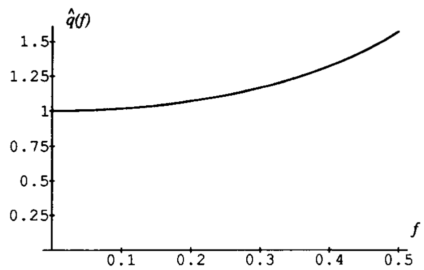

Fig. 6. Frequency response of the digital correction filter for a piecewise constant signal reconstruction.

TABLE II
WORST CASE AND AVERAGE COHERENCE MEASURES BETWEEN $\varphi_1(x) = \text{sinc}(x)$ AND $\varphi_2(x) = \beta^n(x)$, AS A FUNCTION OF THE SPLINE ORDER n

n	$\rho_{12} = \min \lvert\hat{r}_{12}(f)\rvert$	$\lVert r_{12}\rVert_{L_2}$
0	0.636	0.880
1	0.702	0.955
2	0.707	0.971
3	0.707	0.978
4	0.707	0.983
5	0.707	0.986

A potential application of these results is the design of correction filters for improving the rendition of digital images on a display device (e.g., video monitor, film recorder, etc.). We will make the standard assumption that the digital images were acquired using an acquisition procedure that conforms with Shannon's sampling theory and consider the case of a display device that use piecewise constant interpolation. The corresponding basis functions $\varphi_1(x,y) = \text{sinc}(x)\text{sinc}(y)$ and $\varphi_2(x,y) = \beta^0(x)\beta^0(y)$ are separable in the x and y coordinates (x and y represent the horizontal and vertical spatial dimension, respectively). We can therefore use our theory to derive a separable correction filter that is implemented by successive 1-D processing along the rows and the columns of the image. We find that the Fourier transform of the resulting 1-D digital filter is

$$\hat{q}(f) = \frac{1}{\text{sinc}(f)}, f \in \left[-\frac{1}{2}, \frac{1}{2}\right]. \quad (52)$$

This function is plotted in Fig. 6. The effect of this filter is to enhance higher spatial frequencies, which corresponds to a special form of image sharpening.

D. Gaussian-Like Acquisition Device

As our last example, we consider the case of an acquisition device that has a Gaussian-like response. To simplify matters, we assume that the impulse response can be represented by a B-spline of order p: $\varphi_1(x) = \beta^p(x)$, which is a good approximation of a Gaussian, especially for higher order splines. Based on an asymptotic result in [22], we have the following Gaussian approximation

$$\beta^p(x) \cong \frac{1}{\sqrt{2\pi}\sigma_p} \exp\left(-\frac{x^2}{2\sigma_p^2}\right), \qquad \sigma_p = \sqrt{\frac{(p+1)}{12}} \quad (53)$$

which improves rapidly for increasing values of p (for $p = 3$, the approximation error is already less than 1%).

TABLE III
WORST CASE AND AVERAGE COHERENCE MEASURES BETWEEN $\varphi_1(x) = \beta^p(x)$ AND $\varphi_2(x) = \beta^3(x)$, (CUBIC SPLINE) AS A FUNCTION OF THE SPLINE ORDER P

p	σ_p	$\rho_{12} = \min \lvert\hat{r}_{12}(f)\rvert$	$\lVert r_{12}\rVert_{L_2}$
2	0.5	0.995	0.999
3	0.577	1	1
4	0.645	0.997	0.999
5	0.707	0.991	0.998
6	0.764	0.983	0.997
7	0.816	0.975	0.996
8	0.866	0.967	0.995
9	0.913	0.958	0.994

We also choose to represent our signals using splines of order n with $\varphi_2(x) = \beta^n(x)$. The corresponding cross-correlation sequence is

$$a_{12}(k) = b^{p+n+1}(k) := \beta^{p+n+1}(k). \quad (54)$$

The optimal correction operator $q = (b^m)^{-1}$ is the so-called direct B-spline filter of order $m = p + n + 1$, which has been shown to be stable for any value of m [5]. This filter can be implemented using the fast recursive algorithm described in [23].

The spectral coherence function for this example is given by

$$\hat{r}_{12}(f) = \frac{B_1^{n+p+1}(f)}{\sqrt{B_1^{2n+1}(f) B_1^{2p+1}(f)}} \quad (55)$$

where $B_1^n(f)$ denotes the Fourier transform of a discrete B-spline of order n. The corresponding worst case and average performance measures for $n = 3$ (cubic splines) and various values of p are given in Table III. Obviously, for $n = p = 3$, $V_1 = V_2$ and we get the ideal least squares solution. For higher values of p, there is a slight but progressive degradation.

VI. CONCLUSION

We have presented a sampling procedure that allows a rather general specification of the approximation space and also takes into account the characteristics of the acquisition device. The approximation space is usually determined by the digital-to-analog conversion algorithm; for example, zero order splines in the case of a piecewise constant interpolation. The only addition to the standard procedure is a digital correction filter. This technique should therefore be applicable to most practical situations.

In this study, sampling has been considered from the point of view of signal approximation. No special constraint, such as bandlimitedness, is imposed on the input signal. Our only requirement is that output of the acquisition device remains unchanged if the signal approximation is re-injected into the system (consistent measurements). The present formulation is general in the sense that it includes least squares approximation as a particular case. Moreover, it provides a restatement of Shannon's sampling theorem for real measured signal values; i.e., samples obtained after convolution with the impulse response of the sensor. Another important aspect of this theory is the issue of performance. The spectral coherence function has been introduced precisely for that purpose; it can be used to obtain a quantitative comparison with the optimal least squares solution.

One may be tempted to view the present algorithm as a special type of inverse filtering or deconvolution technique. The main difference with those methods is that our approach combines the task of signal approximation and correction for sensor distortions. Moreover, the resulting algorithm is digital although the problem is initially formulated in the continuous signal domain. In this sense, the present formulation provides a proper discretization of an analog deconvolution problem.

Finally, there are several related problems that could be investigated in the future. First, the present scheme does not take into account measurement noise. The problem of additive noise could in principle be dealt with using an approach similar to the Wiener filter [8]. Second, there are cases in which the signal recovery problem may be ill-posed; i.e., it may be difficult (or even impossible) to compute the inverse discrete convolution operator $(a_{12})^{-1}$. Generalized inverse or regularization techniques could be developed to deal with such instabilities.

References

[1] C. E. Shannon, "Communication on the presence of noise," in *Proc. IRE*, vol. 37, Jan. 1949, pp. 10–21.

[2] P. L. Butzer, "A survey of the Whittaker–Shannon sampling theorem and some of its extensions," *J. Math. Res. Exposition*, vol. 3, pp. 185–212, 1983.

[3] A. J. Jerri, "The Shannon sampling theorem—Its various extensions and applications: A tutorial review," *Proc. IEEE*, vol. 65, pp. 1565–1596, 1977.

[4] A. Kohlenberg, "Exact interpolation of band-limited functions," *J. Appl. Physics*, vol. 24, pp. 1432–1436, 1953.

[5] A. Aldroubi, M. Unser, and M. Eden, "Cardinal spline filters: Stability and convergence to the ideal sinc interpolator," *Signal Processing*, vol. 28, pp. 127–138, Aug. 1992.

[6] I. J. Schoenberg, "Contribution to the problem of approximation of equidistant data by analytic functions," *Quart. Appl. Math.*, vol. 4, pp. 45–99, 112–141, 1946.

[7] I. J. Schoenberg, *Cardinal Spline Interpolation*. Philadelphia, PA: Society of Insdustrial and Applied Mathematics, 1973.

[8] W. M. Brown, "Optimal prefiltering of sampled data," *IRE Trans. Inform. Theory*, vol. IT-7, pp. 269–270, 1961.

[9] R. Hummel, "Sampling for spline reconstruction," *SIAM J. Appl. Math.*, vol. 43, pp. 278–288, 1983.

[10] M. Unser, A. Aldroubi, and M. Eden, "Polynomial spline signal approximations: Filter design and asymptotic equivalence with Shannon's sampling theorem," *IEEE Trans. Inform. Theory*, vol. 38, pp. 95–103, Jan. 1992.

[11] A. Aldroubi and M. Unser, "Sampling procedures in function spaces and asymptotic equivalence with Shannon's sampling theory," *Numer. Funct. Anal., Optimiz.*, vol. 15, pp. 1–21, Feb. 1994.

[12] H. Ogawa, "A unified approach to generalized sampling theorems," in *Proc. Int. Conf. Acoust., Speech, Signal Processing* (Tokyo, Japan), 1986, pp. 1657–1660.

[13] ——, "A generalized sampling theorem," *Elect., Commun. in Japan*, vol. 72, pt. 3, pp. 97–105, Mar. 1989.

[14] S. G. Mallat, "A theory of multiresolution signal decomposition: The wavelet representation," *IEEE Trans. Pattern Anal. Mach. Intell.*, vol. 11, pp. 674–693, 1989.

[15] ——, "Multiresolution approximations and wavelet orthogonal bases of $L^2(R)$," *Trans. Am. Math. Soc.*, vol. 315, pp. 69–87, 1989.

[16] A. Aldroubi and M. Unser, "Families of multiresolution and wavelet spaces with optimal properties," *Numer. Funct. Anal., Optimization*, vol. 14, pp. 417–446, 1993.

[17] M. Unser, A. Aldroubi and M. Eden, "The L_2 polynomial spline pyramid," *IEEE Trans. Pattern Anal. Mach. Intell.*, vol. 15, pp. 364–379, Apr. 1993.

[18] A. Papoulis, *Signal Analysis*. New York: McGraw-Hill, 1977.

[19] J. G. Proakis and D. G. Manolakis, *Introduction to Digital Signal Processing*. New York: Macmillan, 1990.

[20] M. J. Marsden, F. B. Richards, and S. D. Riemenschneider, "Cardinal spline interpolation operators on l^p data," *Indiana Univ. Math J.*, vol. 24, pp. 677–689, 1975.

[21] I. J. Schoenberg, "Notes on spline functions III: On the convergence of the interpolating cardinal splines as their degree tends to infinity," *Israel J. Math.*, vol. 16, pp. 87–92, 1973.

[22] M. Unser, A. Aldroubi, and M. Eden, "On the asymptotic convergence of B-spline wavelets to Gabor functions," *IEEE Trans. Inform. Theory*, vol. 38, pp. 864–872, Mar. 1992.

[23] ——, "Fast B-spline transforms for continuous image representation and interpolation," *IEEE Trans. Pattern Anal. Mach. Intell.*, vol. 13, pp. 277–285, Mar. 1991.

Michael Unser (M'89–SM'94) received the M.S. (with honors) and Ph.D. degrees in electrical engineering in 1981 and 1984, respectively, from the Swiss Federal Institute of Technology, Lausanne, Switzerland.

He is currently a Visiting Scientist with the Biomedical Engineering and Instrumentation Program, National Institutes of Health, Bethesda, MD, which he joined in 1985. He has also been affiliated with INSERM (French National Institutes of Health and Biomedical Research) since April 1988. His research interests include the application of image processing and pattern recognition techniques to various biomedical problems, multiresolution algorithms, wavelet transforms, and the use of splines in signal processing.

Dr. Unser was awarded the Brown–Bowery Prize in 1984 for his work on texture analysis and automated inspection. He is the author or coauthor of more than 50 papers in professional journals. He serves as an Associate Editor for the IEEE Transactions on Image Processing and is a member of the Multidimensional Signal Processing Committee of the IEEE Signal Processing Society.

Akram Aldroubi received the M.S. degree in electrical engineering in 1982 from the Swiss Federal Institute of Technology, Lausanne. He received the M.S. and Ph.D. degrees in mathematics in 1984 and 1987, respectively, from Carnegie-Mellon University, Pittsburgh, PA.

He is currently a Senior Staff Fellow at the Biomedical Engineering and Instrumentation Program, National Institutes of Health, Bethesda, MD. His research interests include functional analysis, partial differential equations, and signal/image processing.

Dr. Aldroubi is a member of the American Mathematical Society. While at the Swiss Federal Institute of Technology, he was awarded the Rene Cousin Prize for excellence.